NTIA Report 90-255

A New Approach to HF Channel Modeling and Simulation Part II: Stochastic Model

Lewis E. Vogler
James A. Hoffmeyer

U.S. DEPARTMENT OF COMMERCE
Robert A. Mosbacher, Secretary

Janice Obuchowski, Assistant Secretary
for Communications and Information

February 1990

CONTENTS

LIST OF FIGURES

A NEW APPROACH TO HF CHANNEL MODELING AND SIMULATION

PART II: STOCHASTIC MODEL

L. E. Vogler and J. A. Hoffmeyer*

This report is the second report in a series of reports which describe a new and unique approach for modeling either narrowband or wideband high frequency (HF) channels. Although narrowband models of the HF channel have existed for many years, they are applicable to only a limited set of actual narrowband propagation conditions. The need for an HF channel model that is valid for both narrow and wide bandwidths over a more extensive range of propagation conditions motivated the research documented in this series of reports.

The reports in this series describe the development of a channel transfer function for the HF channel that accurately models a wide variety of propagation conditions and can be used for the evaluation of either narrowband or wideband HF systems. Part I of this series of reports described the development of a model that represents the median channel conditions. The present report, Part II of the series, describes the stochastic portion of the model which simulates the time-varying distortion of a transmitted signal due to dispersion, scattering due to irregularities in the ionosphere, Doppler spread and Doppler shift. The development of the stochastic model is described. The model output is compared with measured propagation data obtained on a variety of HF links. The mechanism for this comparison is the channel scattering function which has been found to be an excellent descriptor of the time-varying dispersive HF channel.

Key Words: channel transfer function; HF channel models; HF propagation; scattering functions; spread spectrum communications; wideband HF

1. INTRODUCTION

Skywave transmission of high frequency (HF) communication signals have been effectively utilized since the communications experiments of Marconi in the early 1900's. Currently

---

* The authors are with the Institute for Telecommunication Sciences, National Telecommunications and Information Administration, U.S. Department of Commerce, Boulder, CO 80303-3328

there is renewed interest in this venerable transmission medium especially for military communications. The reasons for this renewed interest in HF include 1) the realization that multi-media transmission networks are needed for transmission of critical national security information, 2) the need for backup systems to meet emergency telecommunications requirements subsequent to natural disasters, and 3) enhanced digital signal and data processing chips and systems permit the development of HF systems having performance far better than HF systems of only a few years ago.

The justification for the use of multi-media transmission networks is that they enhance network survivability and increase the probability that critical message traffic will be successfully received. HF communication systems are particularly relevant to the problem of reliable transmission of such traffic in a stressed environment.

Wideband (of the order of 1-MHz instantaneous bandwidth) spread spectrum HF communications is one exciting example of the impact which digital technology has had in the HF community. The basic concept of wideband HF (WBHF) was first investigated in the late 1960's (Belknap et al., 1968) when the feasibility of automatic compensation for ionospheric distortion was verified using data obtained from wideband (up to 3-MHz) linear frequency modulation (LFM) channel probe measurements. Until recently, however, digital technology did not permit the practical implementation of the necessary compensation circuitry in a real-time signal processing system. Interest in wideband HF technology has increased significantly during the 1980's (Skaug, 1982 and 1984; Salous and Shearman, 1986; Milsom and Slator, 1982; Perry, 1983; Perry et al., 1987; Bello and Fishman, 1989).

The requirement for the use of wide bandwidths in HF systems warrants further discussion. The employment of wideband signals has advantages for both communications and over-the-horizon radar (OTHR) signals if

(1) the HF medium can support the propagation of such signals,

(2) the transmission of such signals does not interfere with other users in the band, and

(3) the effects of external noise and interference in the wideband channel can be mitigated through the use of appropriate signal processing.

For communication systems, the advantages of spread-spectrum technology are well known (Dixon, 1984). These advantages include low-probability-of-intercept (LPI) communications, interference rejection, simultaneous operation of several transmitters in the same frequency band, and resolution of multipath sky-wave returns. For HF radar systems,

the use of wideband spread-spectrum signals results in improved range resolution. Thus, both applications require the use of the widest possible bandwidth for a given path, time of day, season, sunspot number, etc.

The successful development of any new communications capability is dependent upon a thorough understanding of the transmission media. Theoretically one should start with propagation measurements which characterize the channel, and develop a propagation model for that channel. This would be followed by the use of either software simulation or analytical techniques to evaluate the expected performance of alternative communication system designs. The communication system design alternative having the highest simulated performance would then be implemented in hardware. The prototype communications system performance would then be evaluated in a series of representative laboratory and field tests.

There are many uncertainties regarding the attainable performance of either wideband HF communications systems or extended bandwidth OTHR systems. A capability to evaluate the potential performance of such systems without the cost of building the hardware and running extensive field tests is needed (see Figure 1). Theoretical performance assessments can be attained through the use of simulation software. This software includes both software

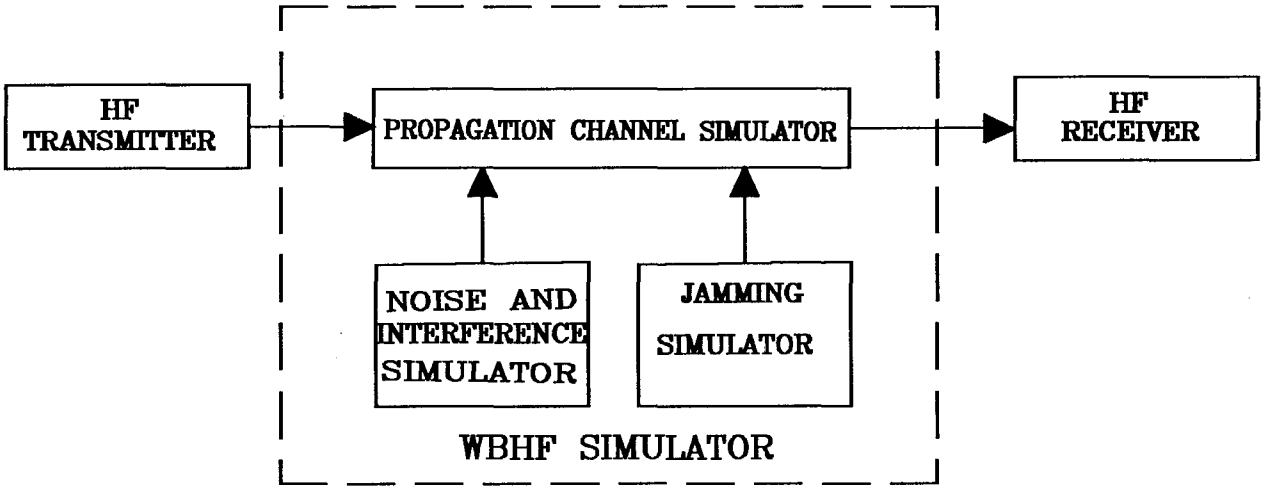

Figure 1. Types of simulators for HF systems testing.

to simulate the perturbations of the HF medium, i.e. simulation of the channel transfer function, and software that simulates the HF communications system itself.

Laboratory testing of advanced technology HF communications systems in the laboratory requires the development of simulators. As depicted in Figure 1, there are three types of simulators required for testing HF communications systems which are designed for operation in a stressed environment: a propagation channel simulator, a noise/interference simulator, and a jamming signal simulator. Each of these simulators must be based on models which have been validated through the use of empirical data. This report is restricted to the discussion of the channel propagation model. Lemmon (1989) describes the noise/interference modeling work which is ongoing at the Institute.

1.1 Restrictions of Existing HF Channel Models

For many years, the high frequency (HF) channel model and channel simulation techniques developed by C. Watterson have been utilized for the laboratory performance evaluation of narrowband HF communication systems. This narrowband model, its implementation in both hardware and software simulators, and the use of these simulators in HF system performance evaluation have been widely reported in the literature (Watterson, 1981 and 1982; Watterson and Coon, 1969; Watterson et al., 1969 and 1970; CCIR, 1974; Ehrman et al., 1982; Mooney, 1985; Girault et al., 1988; McRae and Perkins, 1988; LeRoux et al., 1987). Despite the apparent usefulness of the Watterson HF channel model and simulators which utilize the model there are a number of restrictions on the model. For example, the model is valid only for narrowband (less than 12-kHz) stable channels.

The initial motivation for the development of a new channel model was the bandwidth restrictions of the Watterson model. The Watterson model was validated using 36 minutes of data on a single, 1300-km path (Watterson et al., 1970). The valid bandwidth of the model was found to be 2.5-kHz, 8-kHz, and 12-kHz for the three sample periods in which propagation data were taken during a single day in November 1967. Watterson was quite clear in the restrictions of the channel model that was later promulgated in a CCIR Report (CCIR, 1974). Unfortunately, with the passage of time, many of these restrictions apparently have been forgotten. The model is currently being implemented in a channel simulator with a "24-kHz bandwidth" capability. Although, the machine has the processing capability for a 24-kHz throughput, there is no justification for the extension of the Watterson model beyond the 2.5 - 12-kHz bandwidth originally claimed for the model.

As has been noted by other researchers, there are other restrictions on the general applicability of the Watterson model (LeRoux et al., 1987; CCIR, 1986). The model is representative of the HF channel only when the channel may be considered to be stationary and stable. In the validation of the model, Watterson selected data that "seemed most nearly stationary in terms of fading rates, modal time delays, and average power in the modes" (Watterson et al., 1969). In summary, the model is limited to

- channel bandwidths of 12 kHz or less
- channels having time and frequency stationarity
- channels having negligible delay dispersion (e.g., no spread-F)
- channels having only a low-ray path

The limitations of the Watterson model are recognized in CCIR Report 549-2 (CCIR, 1986) in the following statements:

- "Since the channel model has discrete paths with zero time-spread, while each ionospheric mode always has at least a small time-spread, the accuracy with which the channel model can represent an ionospheric channel decreases with increasing bandwidth."

- ..."The Gaussian-scatter model almost certainly is not valid for all HF ionospheric channels."

Although the existing narrowband models have proven useful, their limitations and the present need for more accurate modeling and simulation of the HF channel provide motivation for the development of a new HF channel model.

1.2 Critical Requirements for a New HF Channel Model

Modeling Dispersion and Scattering Effects.

The ability to accurately represent a wideband (of the order of one MHz) HF channel is a primary requirement for the new HF channel model. The bandwidth restrictions of the Watterson model and the need for simulation of wideband HF channels have led other researchers to propose a new model in which delay is a function of frequency (Barratt and Walton, 1987). Watterson assumed that the propagation delay in a narrowband model is independent of frequency, i.e. there is no dispersion in a narrowband channel. For the wideband case, it is obvious from looking at ionograms (see Wright and Knecht, 1957 for example) that delay time does vary with frequency over the 1-MHz bandwidth of the wideband channel. Typical values of dispersion are a few 10's of μs/MHz for undisturbed midlatitude paths, but have been found to be 240μs /MHz on a midlatitude path during spread-F conditions (Wagner et al., 1989). Although the Barratt and Walton model does add dispersion to the

Watterson model, it does not add the effects of scattering or time smear to the model. The requirement to model both dispersion and scattering is discussed below.

Figure 2 provides examples of two hypothetical ionograms - one for a quiet ionosphere and one for a disturbed ionosphere containing spread-F. For these hypothetical ionograms it is clear that for the narrowband channel (say 3-khz), dispersion is negligible for either the quiet ionosphere or the disturbed ionosphere. Dispersion is not negligible for the wideband channel for either the quiet or disturbed ionospheres. It is also clear, however, that scattering is the dominant effect rather than dispersion in the spread-F channel. These hypothetical ionograms are presented to illustrate the point that it is important to model the scattering (diffuse multipath) propagation effect which is not done in either the Watterson narrowband model or the Barratt and Walton "wideband" model.

Figure 3 is an actual ionogram due to Basler et al. (1987a) which is presented here to demonstrate that the hypothetical ionogram of Figure 2b is not unlike actual ionograms. The ionogram in Figure 3 depicts propagation conditions on a 1913-km one-hop propagation path in Greenland. Although the spreading conditions shown in the ionogram occur more frequently on polar and trans-auroral paths than they do on midlatitude paths, spread-F occurs sufficiently often on midlatitude paths that it dictates the inclusion of scattering conditions or diffuse multipath in any realistic HF channel model - either narrowband or wideband. Milsom and Slator (1982) state that one could expect spread-F conditions over England for approximately 35% of the time during the winter of a year having a minimum sunspot number. Because diffuse multipath caused by scattering due to ionospheric irregularities can have a significant effect on performance of advanced digital HF communications systems, it is important that this channel characteristic be included in either narrowband or wideband models and simulators.

The model described in this report and by Vogler and Hoffmeyer (1988) addresses this key issue of modeling channels of arbitrary bandwidths up to 1-MHz and beyond including the modeling of both dispersion and diffuse multipath scattering.

Modeling Both Gaussian and Non-Gaussian Spectra

The Watterson model is a tap-delay line model whose tap-gain multipliers have a Raleigh amplitude distribution and a uniform phase distribution. The spectra for the tap-gain functions are assumed to be Gaussian. This was later "validated" using data from only a single path and only a few minutes of data collected on a single day (Watterson, et al., 1969). As noted

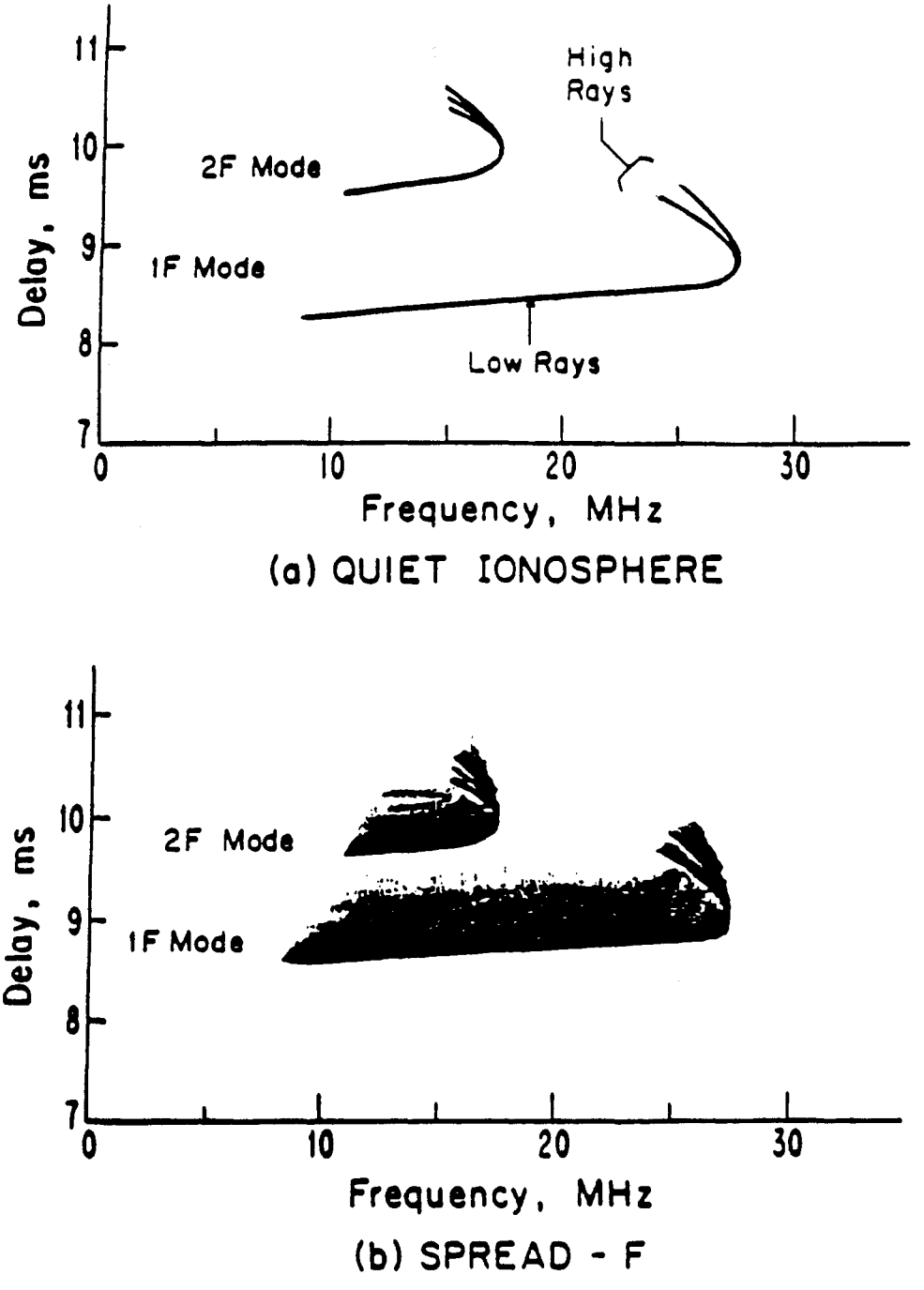

Figure 2. Hypothetical ionogram examples.

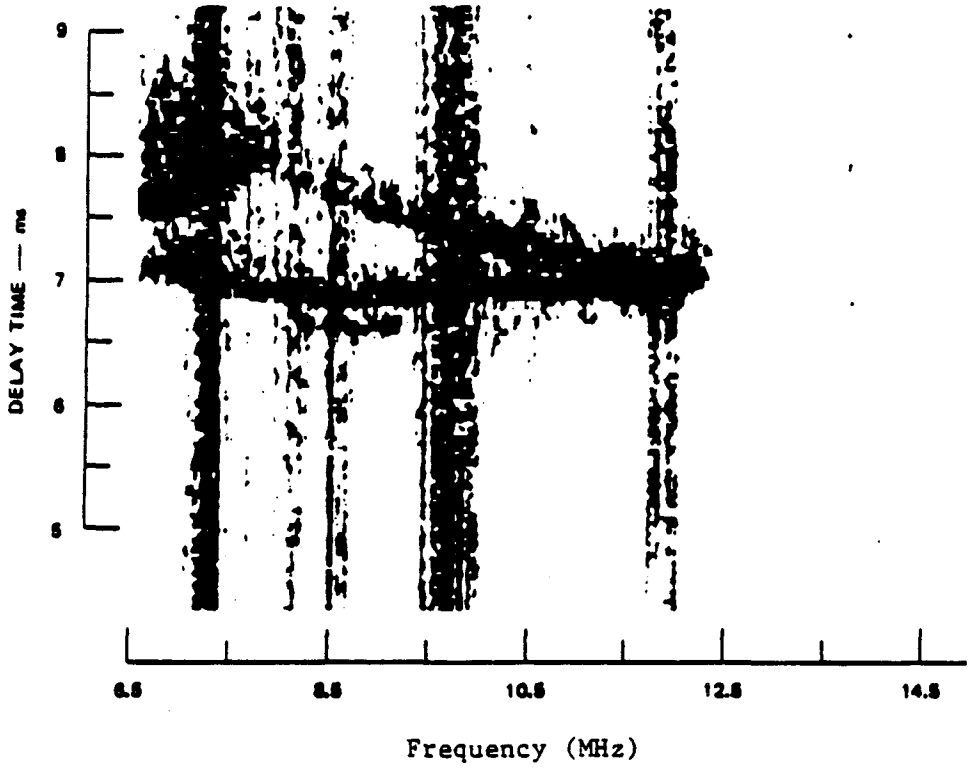

Figure 3. Oblique ionogram from Bassler et al. (1987a, p.44). Recorded on 8 October 1984 at 1901 GMT on a 1913-km path from Narssaruaq-Thule, Greenland.

above, the CCIR (1986) Report 549-2 states that the Gaussian spectra assumption does not hold universally for all ionospheric paths. Serrat-Fernandez et al. (1985) also discuss the need for spectral shapes of the tap-gain functions other than Gaussian. Later sections of this report address our approach for modeling this variable.

1.3 Steps in the Development of a New HF Channel Model

The bandwidth limitation of the Watterson model and the growing interest in wideband HF communications were the initial motivating factors for a study conducted at the Institute in 1986 which addressed the feasibility of developing a wideband HF channel simulator. This study (Hoffmeyer and Nesenbergs, 1987) concluded that the development of a new channel simulator must be preceded by the development of a new HF channel model which must be based on new wideband HF channel propagation measurements. At the time of the study, few wideband channel measurements had been reported in the literature. Since that time, the Naval Research Laboratory has conducted a number of wideband (250-kHz and 1-MHz) HF propagation measurement experiments useful in the channel model development process (Wagner et al., 1989; Wagner, 1987; Wagner et al., 1987a, 1987b, and 1988; Wagner and Goldstein, 1985; Wagner et al, 1983).

The HF channel propagation experiments conducted by Wagner using a 1-MHz HF channel probe (Wagner et al., 1983) and by Basler using a 20-kHz channel probe (Basler et al., 1987a, 1987b, and 1988) have provided data which are invaluable in the development of a new HF channel model. These data were used in both the development of the deterministic portion of the new model (Vogler and Hoffmeyer, 1988) and in the development of the stochastic portion of the model which is described in the following sections.

2. SCATTERING FUNCTION

The principal stochastic effects that the HF simulation model must describe are the delay time spread and the Doppler frequency spread. The channel scattering function (Proakis, 1983; pp. 461-463) relates these quantities and provides the means by which the signal energy distribution may be represented in graphical form. The delay spread characterizes the spread in time of a transmitted pulse, and the Doppler spread serves in a similar manner as a measure of frequency variation.

The spreads are usually considered to be caused by specular reflections plus scattering from irregularities and random refractive index fluctuations of the ionosphere. Thus, the deterministic component of the delay spread is the result of dispersion arising from the reflection of different frequency components at different heights of the ionospheric layer. In addition to this is a stochastic component caused by the scattering process. For the purposes of simulation, only an overall spread is of importance, and it is not necessary to differentiate between the deterministic and stochastic components.

The scattering function $S(\tau, f_D)$, relating the signal amplitude dependence on delay time τ and Doppler frequency f_D can be thought of as the power spectrum of contributions in the delay interval $\tau+\Delta\tau$ that cause a relative frequency shift in the range $f_D+\Delta f_D$. It is evaluated as the Fourier transform over time t of the (complex) received signal auto-correlation function $\hat{C}(\tau, f_s; t)$:

$$S(\tau, f_D)=\int_{-\infty}^{+\infty} \hat{C}(\tau, f_s; t)\exp(-i2\pi f_D t)dt \qquad (1)$$

where f_s is the Doppler shift for a particular mode. The specific form given to $\hat{C}$ determines the shape and extension of the delay and Doppler spreads and is discussed in the next subsection.

2.1 The function $\hat{C}(\tau, f_s; t)$

The analytic form of the auto-correlation $\hat{C}$ is assumed to be the product of a delay amplitude factor $T(\tau)$, a correlation factor C(t) showing the amplitude dependence on the time lag t, and a function $\varphi_s(\tau, f_s; t)$ representing the phase portion of the complex signal:

$$\hat{C}(\tau, f_s; t)=T(\tau)\, C(t) \exp[i\varphi_s(\tau, f_s; t)] \qquad (2)$$

For a Watterson (narrowband) model (Watterson et al., 1969; pp. 20 and 29),$T(\tau)$ is simply a delta function evaluated at a particular choice of τ, $\delta(\tau-\tau_o)$; the factor C(t) is assumed to have a Gaussian form and $\varphi_s=2\pi f_s t$ is the phase at an arbitrarily chosen Doppler shift f_s.

When considering wideband simulation models, the distortion of the transmitted pulse caused by dispersion and by scattering from ionospheric irregularities results in a spread of

the energy in the pulse over an interval of delay time τ. In this case $T(\tau)$, rather than being a delta function, becomes a shape factor giving a measure of the delay spread in the received pulse. Expressions for the equivalent of $T(\tau)$ based on a thin screen scatter model have been developed by Basler et al. (1987a). This development describes the physical processes involved in turbulence and scattering theory and is valuable in understanding the effects of the medium on propagation. However, for our present simulation model, we have assumed a much simpler form for the delay factor, but a form with enough versatility to characterize the key features of the physically-based expressions from scatter theory. This should be adequate as long as the simulation of channel effects is our goal.

2.1.1 Delay Amplitude factor $T(\tau)$.

The expression used for $T(\tau)$ in the present model is

$$T(\tau) = A y^{\alpha} \exp[\beta\ (1 - y)],\ \alpha,\ y \geq 0 \qquad (3)$$

$$y = (\tau - \tau_L) / (\tau_c - \tau_L),$$

where τ_c denotes the delay time associated with the carrier frequency and τ_L is the lower or minimum value of the delay. The amplitude A, together with the total spread $\sigma_\tau=(\tau_U - \tau_L)$ and subinterval $\sigma_c=(\tau_c - \tau_L)$, are three parameters that can be chosen to generate the variety of shapes indicated by wideband HF measurements. For the computer program that implements the model in software and that is used to simulate actual measured scatter functions in a later section, the three parameters are read in from the data and determine the values of α and β according to the following equations.

(I) For $0 \leq y \leq 1$ ($\tau_L \leq \tau \leq \tau_c$):

$$\alpha = \{(1-y_2) \ln A_1 - (1-y_1) \ln A_2\} / d \qquad (4a)$$

$$\beta = (\ln y_1 \ln A_2 - \ln y_2 \ln A_1) / d \qquad (4b)$$

$$d = (1-y_2) \ln y_1 - (1-y_1) \ln y_2 \qquad (4c)$$

$$y_1 = 0.01, y_2 = 0.5, A_1 = A_{fl}$$

$$A_2 = \exp\left[(\ln A_1)(1 - y_2 + \ln y_2) / (1 - y_1 + \ln y_1)\right] \tag{4d}$$

and A_{fl} denotes the signal floor or receiver threshold, below which the signal amplitude is essentially zero. The A_i, y_i pairs in (4a–c) refer to amplitudes read off at particular y values, and if it were desired to fit a specific scatter function more closely, two pairs of actual measured values could be used. However, the specific values chosen in (4d) are the ones used in the current computer program, as is the equation for A_2 which results in the condition, $\alpha = \beta$. These choices simplify the procedure for determining $T(\tau)$.

(II) For $y > 1$ ($\tau > \tau_c$) :

$$\alpha = \left\{ (y_2 - 1) \ln A_1 - (y_1 - 1) \ln A_2 \right\} / d \tag{5a}$$

$$\beta = (\ln y_2 \ln A_1 - \ln y_1 \ln A_2) / d \tag{5b}$$

$$d = (y_2 - 1) \ln y_1 - (y_1 - 1) \ln y_2 \tag{5c}$$

$$y_1 = (y_2 + 1) / 2, y_2 = \sigma_\tau / \sigma_c,$$

$$A_1 = 0.5, A_2 = A_{fl} / A, \tag{5d}$$

where A, σ_τ and σ_c are the three parameters mentioned above obtained from the measured scatter function, and the A_i, y_i pairs refer to fitting values in the region $y > 1$. Because we stipulate that the peak value of $T(\tau)$ occurs at $\tau = \tau_c$ or $y = 1$, we must impose the condition that the ratio α / β as obtained from (5) must not exceed unity. This follows from the fact that the maximum of the function given by (3) is at $y = \alpha / \beta$.

The value of τ_c is determined from the delay - frequency relation derived in Vogler and Hoffmeyer (1988). It depends on the carrier frequency f_c, the path distance D, and the ionospheric physical parameters: penetration frequency f_p, layer height h_o, and layer thickness σ. The delay is found as a solution of

$$f_c = f_p \left[\left\{1 + (D / 2\bar{h})^2\right\} / \left\{1 + e^{(h_o - \bar{h})/\sigma}\right\}\right]^{\frac{1}{2}} \tag{6}$$

$$\bar{h} = \left\{(c\tau_c / 2)^2 - (D / 2)^2\right\}^{\frac{1}{2}}$$

where c denotes the free - space speed of light. For an oblique path in which $D > 0$, (6) gives two values of τ_c --one for the high- and one for the low-ray. It would simplify the simulation process if the same set of stochastic parameters A, σ_τ, and σ_c could be used for both rays. However, measurements studied so far show no indication of this, and independent sets are used in the comparisons later on.

2.1.2. Correlation Factor C(t) .

The correlation factor determines the shape and extent of the Doppler spread and has been discussed at length in connection with narrowband HF simulation models. A Gaussian form is usually adopted although this has been validated only under quite restricted conditions, i.e., very narrow bandwidths and a stable ionosphere. In fact recent measurements have suggested a different shape might be more appropriate in many situations (Basler et al., 1987a). As a consequence, the present software simulation model provides two alternatives for the shape of the Doppler spread: (1) a Gaussian shape, and (2) a "peak" shape arising from an exponential auto-correlation function.

The Gaussian shape may be obtained from

$$C(t) = A\,\sigma_f \exp\left[-\pi\,(\sigma_f\, t)^2\right] \tag{7}$$

$$\sigma_f = \sigma_D \left[-\ln\left(A_{fl} / A\right) / \pi\right]^{-1/2}$$

where σ_D is the user selected half-width of the Doppler spread at the receiver floor A_{fl}. Substitution of (7) into (1), with $T(\tau) = \delta(\tau - \tau_o)$ and $\varphi_s = 0$, produces the Gaussian-shaped Doppler spread of the narrowband Watterson model (Watterson et al., 1969; p. 29),

$$\left| S(\tau, f_D) \right| = A \exp\left[-\pi \left(f_D / \sigma_f \right)^2 \right], \ \tau : \text{constant} \tag{8}$$

The generation of normally distributed random variables for the scatter process can be accomplished in various ways, but one of the most useful is the log-and-trig method (Mihram, 1972; p. 128). This also has a physical justification if the received signal is assumed to be Rayleigh distributed with uniform phase. From two independent random variables, one Rayleigh and the other uniformly distributed over 0 to 2π, one can obtain a pair of independent, standardized random normal variates from the expressions

$$z_1 = (-2 \ln u_1)^{1/2} \cos(2\pi u_2)$$

$$z_2 = (-2 \ln u_1)^{1/2} \sin(2\pi u_2) \tag{9}$$

where u_1, u_2 are two independent uniformly distributed random variables defined on the interval (0, 1). The efficiency of this method depends, of course, on the special function subroutines.

The second Doppler spread shape that is suggested by measurements of scatter functions arises from an exponential correlation factor.

$$C(t) = \begin{cases} A \sigma_f \exp(-\sigma_f t), & t \geq 0 \\ 0. & t < 0 \end{cases} \tag{10}$$

$$\sigma_f = 2\pi\sigma_D \left(A_{fl} / A \right) \left[1 - (A_{fl} / A)^2 \right]^{-1/2}$$

where σ_D, A, and A_{fl} are user selected values with the same meanings as before. From (1), with $\hat{C} = C$, the Fourier transform of (10) centered at an arbitrary Doppler shift of f_s results in (Campbell and Foster, 1948; p. 45)

$$\left| S(\tau, f_D) \right| = \sigma_f \, [2\pi(f_D - f_s)^2 + \sigma_f^2]^{-1/2}, \ \tau\text{: constant.} \tag{11}$$

The generation of random variables having an exponential auto-correlation function is described in Naylor et al. (1966; p. 120). The variates x are given by

$$x_n = u_n + (x_{n-1} - u_n)\,\lambda, \ n = 1, 2, 3, \ldots$$

$$x_o = (1 - \lambda)\, u_o, \ \lambda = \exp[-(\Delta t)\,\sigma_f] \tag{12}$$

where (Δt) is the time increment and the u_n are independent uniformly distributed random variables defined on the interval$(-1/2, +1/2)$. The correlation coefficient of lag m is then

$$\rho\ (m) = \exp[-m\,(\Delta t)\,\sigma_f]. \tag{13}$$

2.1.3 Phase Function $\varphi_s(\tau, f_s; t)$.

Variations over time of the physical parameters of the ionosphere result in variations (from a changeless medium) of the signal frequency components. These Doppler effects are characterized analytically as time derivatives of the received phase at a constant value of τ. For a simulation model, the phase function φ_s in (2) can be approximated by

$$\varphi_s(\tau, f_s; t) = \varphi_{so} + \varphi'_s t + \left(\frac{1}{2}\right) \varphi_s'' \, t^2 \tag{14}$$

where φ_{so} is constant for a given τ and the primes denote derivatives with respect to time.

The first derivative $\varphi_s' = 2\pi f_s$ is designated the Doppler shift of the mode and is a measure of the rate of change of the ionospheric physical parameters. It is usually thought of as related to a change in layer height, but it also may be associated with a changing electron density. Values of f_s can vary from zero to plus or minus tens of Hertz, depending on the rapidity with which the physical parameters change over time, and in simulation, the shift is usually one of the arbitrarily chosen inputs.

If the second derivative of φ_s is non-zero, i.e., the Doppler shift changes with time, a plot of the scatter function displays the "slanted" ridges associated with a more unstable ionosphere. In the present model, this is approximated by a linear relationship between delay and Doppler and the phase function has the form

$$\varphi_s (\tau, f_s; t) = 2\pi \left[\varphi_o + \left\{ f_s + b(\tau_c - \tau) \right\} t \right] \tag{15a}$$

$$b = (f_{sL} - f_s) / (\tau_c - \tau_L) \tag{15b}$$

where f_{sL} is the Doppler shift at the delay τ_L. As can be seen from the curly brackets in (15a), b is simply the slope of the "slanted" ridge, and the definition used in (15b) was chosen for convenience in comparing with actual measured scatter functions.

There are, of course, many configurations of Doppler shift versus delay other than the straight-line "slants" modeled by (15). These could be simulated, for instance, by continuing the Taylor series expansion in (14); however, the added complexity involved in calculations and required input is probably not worth the effort. It also appears that, as the ionosphere becomes more and more unstable, random scattering becomes dominant and masks any clear-cut configuration. In the extreme case, the shapeless patterns typified by spread -F conditions occur, and detailed representations have little meaning.

In the following section, simulations of scatter functions using the equations discussed above are compared with measured scatter functions for a variety of channel conditions. Since little other information was available, many of the input parameters for the model were estimated from the measurement plots themselves. In normal usage, each of the parameters would be given an average value (or range of values) typical of the location, time of day and year, and geophysical conditions governing the channel under investigation.

3. COMPARISONS OF MODEL AND MEASUREMENTS

The comparisons of this section were chosen to represent a variety of locations and of ionospheric states. Equatorial, mid-latitude, and polar paths are presented during both quiet and turbulent conditions in order to show the variability encountered in measured scatter functions. Delay spreads range from a few microseconds to over 2 milliseconds, and Doppler spreads vary from 0.1 to over 40 Hz.

The input parameters used in the equations of Section 2 that simulate the scatter function are listed in Table 1 of the Appendix for each of the comparisons shown here. In some cases an ionogram was available from which the layer parameters f_p, σ, and h_o could be determined; when there was no ionogram, values that seemed reasonable were assumed. The number of modes in a simulation can be one, two, or three and if no high-ray return is present, this is indicated in the table by a row of zeros.

The measured scatter functions are from two sources:

(1) an HF Channel Probe with a 20 kHz bandwidth developed by SRI International (Basler et al., 1987a);

(2) an HF Channel Probe with up to 1 MHz bandwidth developed at the Naval Research Laboratory (Wagner et al., 1988)

Both probes use a technique involving pseudorandom noise phase modulation, and both include an HF sounder in conjunction with the probe. The sounder serves to establish the frequencies of interest at which the probe is set to gather data needed for the calculation of scatter functions. As mentioned above, plots of data from the sounder-i.e., ionograms-are useful in the comparisons in order to determine simulation model values for the quantities f_p, σ, and h_o.

3.1 Equatorial Long Path

Figure 4a shows the plot of a scatter function from a 2158-km east-west path between Truk and Majuro in the Pacific Ocean. The measurements were taken in July 1986 and are representative of late night hours. The upper part of the figure is a contour plot of the data, and the middle portion displays a theoretical scatter function developed by Basler et al. (1987a). The two smaller plots at the bottom show profiles of the Doppler frequency (at the peak amplitude) and delay time (at 0 Hz Doppler frequency). The delay and Doppler spreads are 0.88 ms and 4 Hz, respectively.

The simulation in Figure 4b is a three-dimensional representation of the present model using the input parameters in Table 1 of the Appendix. The amplitude is scaled to peak at 10 dB rather than the 30 dB shown in the data plot, but the delay spread profile is similarly shaped. The extent of the spread is verified by an ionogram taken about this time showing the "fuzzy" character of the trace near the carrier frequency of 11 MHz.

3.2. Polar Long Path

An example of a scatter function from a 1913-km north-south path in the polar region over Greenland is shown in Figure 5a (Basler et al., 1987a). The measurements were taken in March 1985 and show returns from an E-layer and from the low- and high-rays of the F-layer. Again, the middle plot shows the SRI-developed theoretical function and the lower plots are profiles of the delay and Doppler spreads. Considerably more movement in the scattering is evident here than in the equatorial case shown previously, causing an extensive Doppler spread. Also, the carrier frequency is close enough to the junction frequency to cause overlap in the low- and high-ray returns from the F-layer.

The simulation in Figure 5b lacks the small scale random fluctuations of the data contours but agrees in general with the spread dimensions in both delay time and Doppler frequency. The shape of the narrow-peaked Doppler spread, especially noticeable in the F-layer low-ray return, is the result of using the exponential correlation factor defined by (10). The Gaussian form of eq. (7) produces a more rounded shape than the exponential form, and the two are compared in Figure 5c. The sharper peak seems to be a characteristic of many of the SRI data measurements and, for this reason, is included as part of the present simulation model.

3.3 Mid-Latitude Short Path

If the physical constituents of the ionosphere vary over time in a nonlinear manner, i.e., if φ_S'' in (14) is non-zero, the scatter function exhibits a τ dependence in the Doppler frequency. This is illustrated in Figure 6a for some 1983 winter afternoon measurements over a 126-km path in southern California (Wagner et al., 1989). The plot represents 1-hop F-layer returns from the low-ray ordinary and extraordinary modes. (The sparse, low-level return on the left side is a spurious result cause by an equipment misadjustment.)

The simulation in Figure 6b reproduces the main characteristics of the measured scatter function and shows the f_D, τ dependence in both modes. The delay scale in (a) has an arbitrary

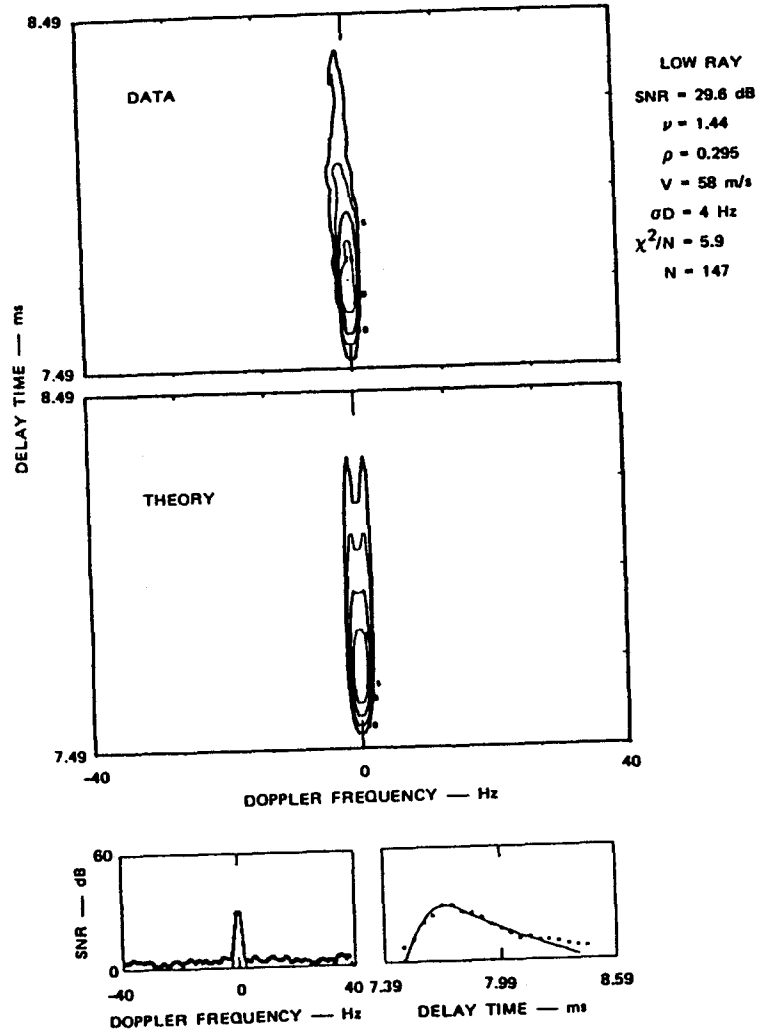

(a)

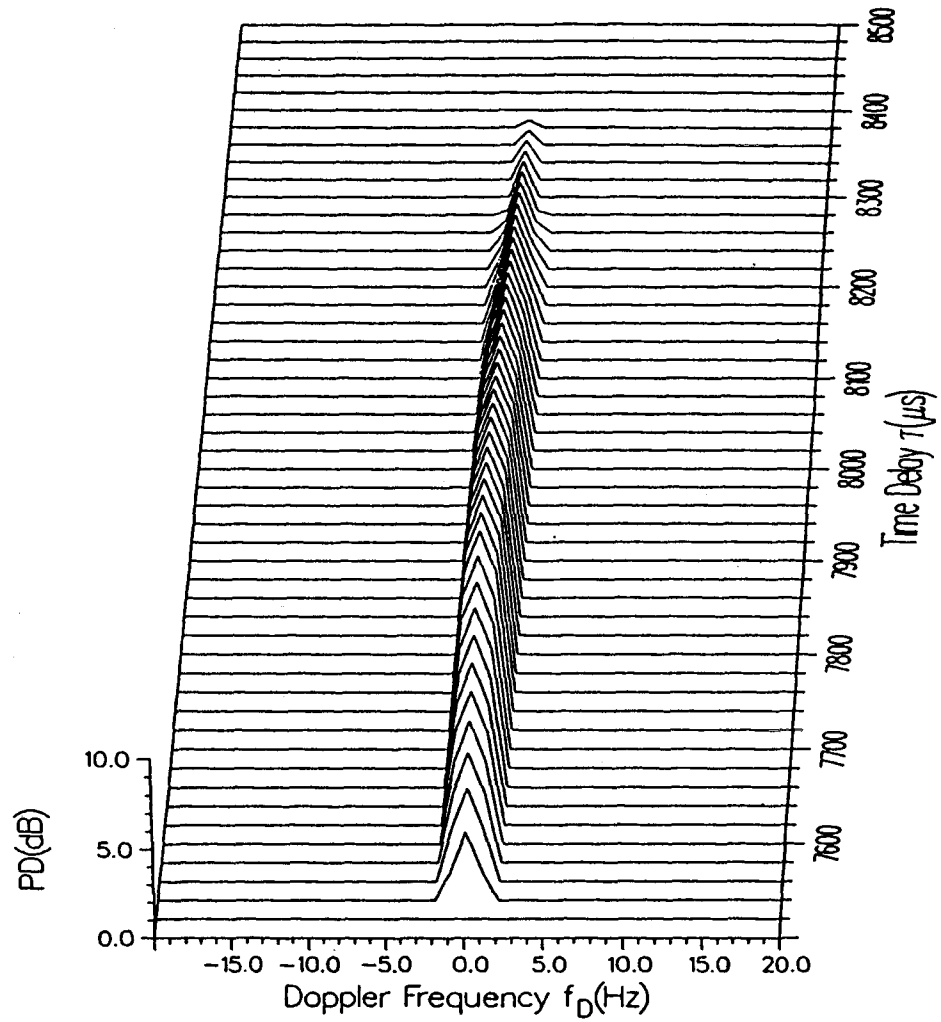

(b)

Figure 4. Scatter function from 2158-km equatorial path. (a) Data from Basler et al. (1987a; p. 137). Middle plot is SRI - developed theory. Lower two plots depict Doppler and delay profiles through the peak amplitude. (b) Simulation from present model; amplitude has been scaled by a factor of 6.

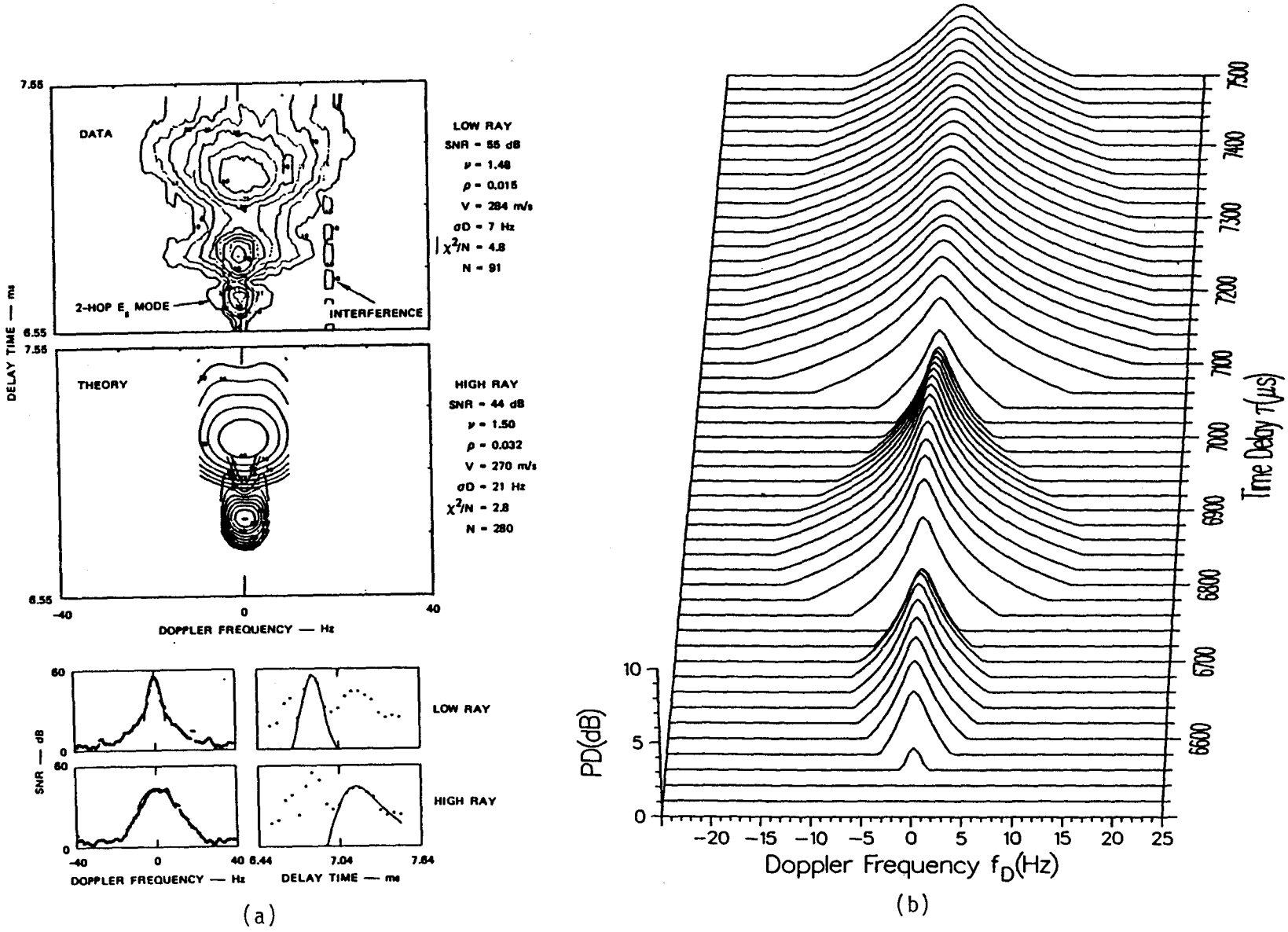

Figure 5. Scatter function from 1913-km polar path. (a) Data from Basler et al. (1987a; p. 79). Middle plot is SRI - developed theory. Lower two plots depict Doppler and delay profiles through the peak amplitude. (b) Simulation from present model; amplitude has been scaled by a factor of 6.

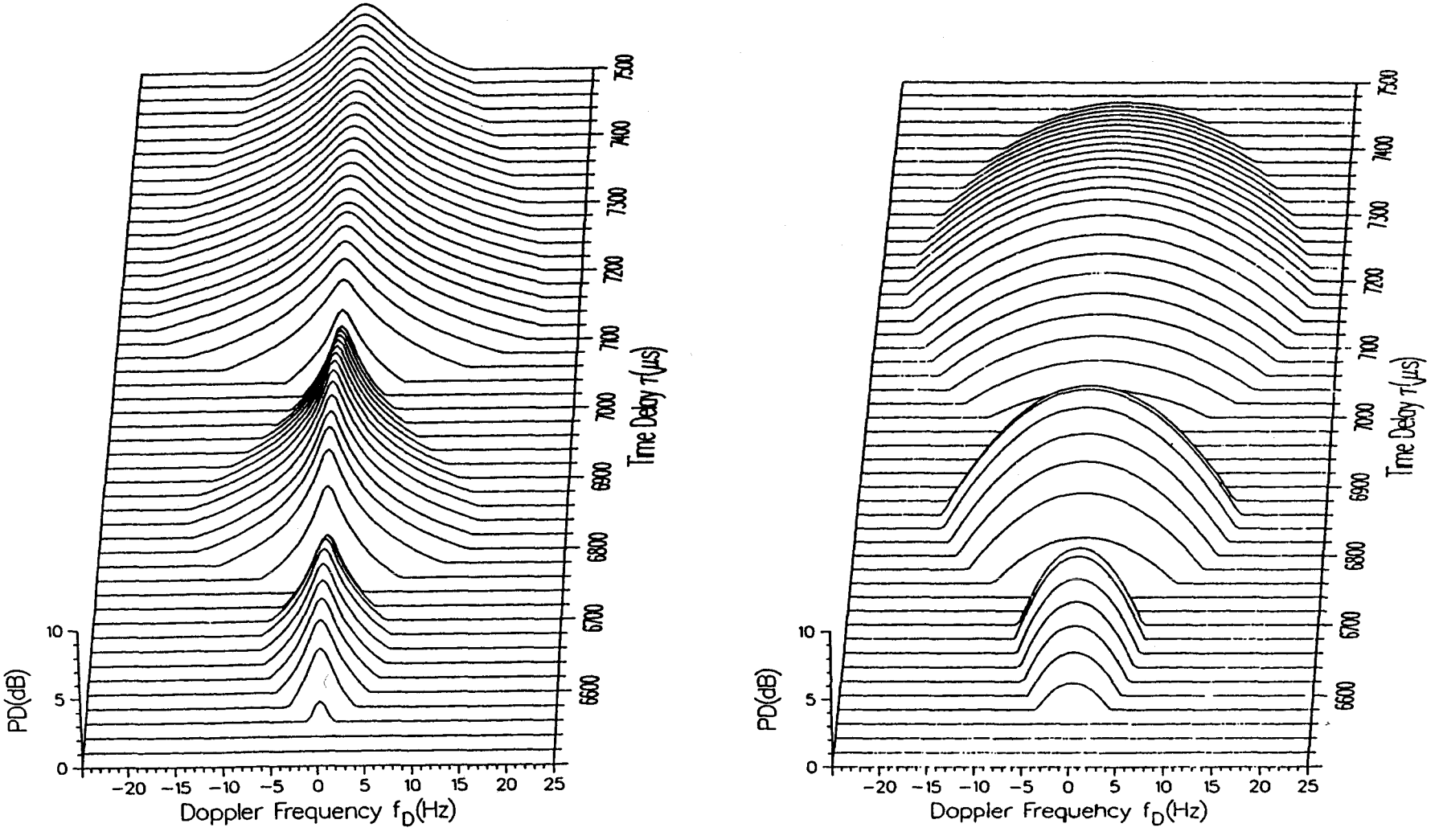

Figure 5c. Scatter functions using the exponential (left) and Gaussian (right) correlation factors. Input parameters are the same as in Figure 5b.

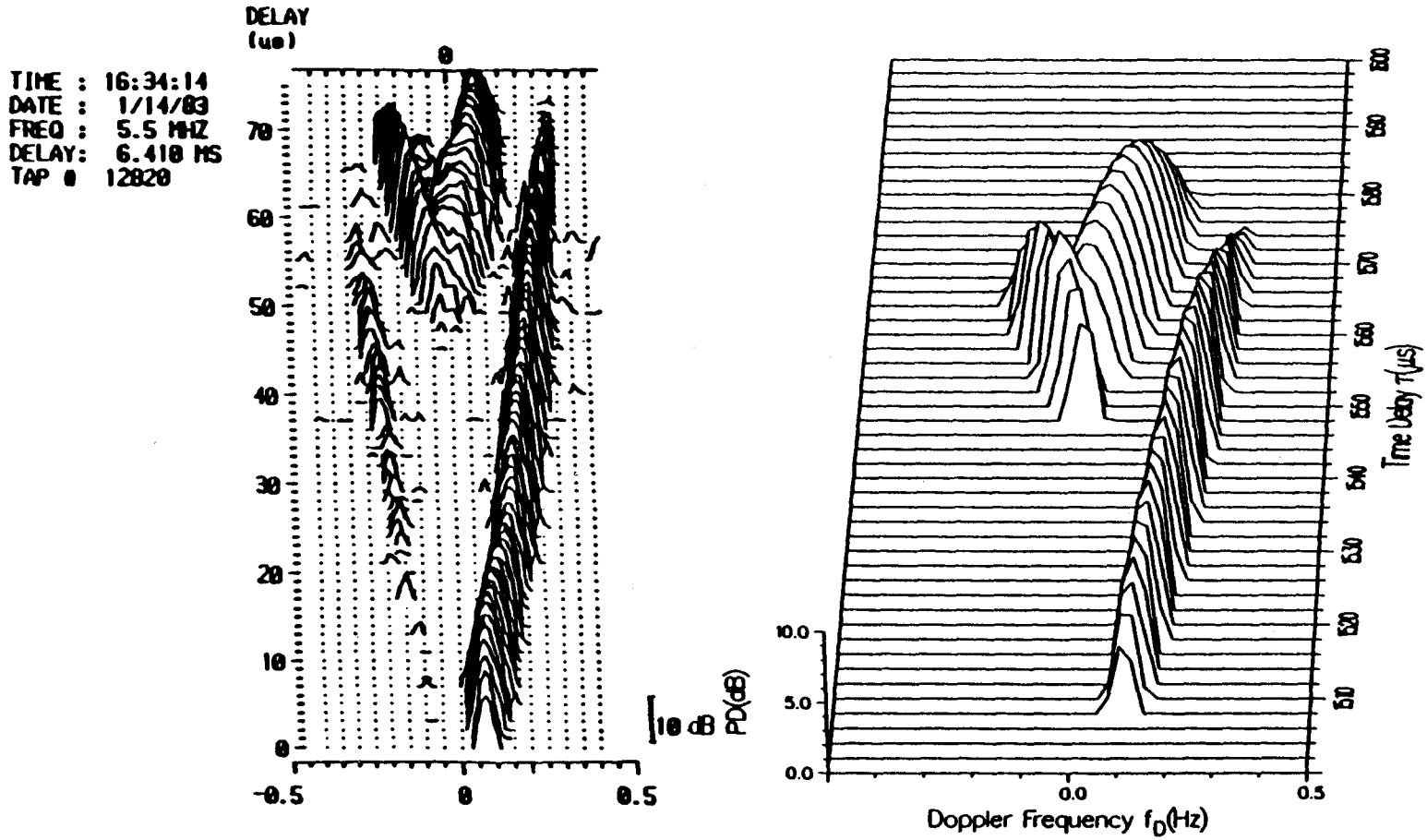

(a) Data from Wagner et al. (1989)

(b) Simulation

Figure 6. Scatter function from 126-km midlatitude path.

zero offset. Notice that the ridge representing the (measured) ordinary return in Figure 6a departs slightly from the linear and, thus, differs to this extent from the simulated return. As mentioned in the last section, a closer fit could be obtained, but at the expense of added complexity to the model.

3.4 Auroral Short Path

The simulation of spread-F conditions in the model is accomplished by introducing a random number factor that multiplies the nonspread return. Input parameters are entered just as in the normal case (see entries for Figures 7 and 8 in Table 1 of the Appendix), and the calculated scatter function points are multiplied by the random factor. Figure 7a shows the measured scatter function from an 88-km east-west path in Alaska (Wagner et al., 1989); the data were taken during a night in May 1988. The conditions were that of severe spread-F, and there was no apparent mode or multipath structure.

The simulation of Figure 7b has assumed returns from a single low ray with delay and Doppler spreads as given in Table 1 of the Appendix. The arbitrary value of $\sigma_c = 400\mu s$ was chosen to be small compared to the overall delay spread ($\sigma_\tau = 1900\mu s$) because this results in a broad Doppler spread at the lowest delay time. The simulation appears to give an adequate reproduction of the shape of the measured scatter function.

After about an hour, conditions on the Alaska path had changed and the severe spread-F had somewhat subsided. A scatter function measured at this time is shown in Figure 8a. It can be seen that the extent of the delay spread is about the same as before (notice that the carrier frequency has been changed), but the Doppler spread is considerably less.

As before, the simulated scatter function in Figure 8b adequately reproduces the measured shape in both delay and Doppler. Furthermore, it is interesting to note that spread-F conditions are relatively easy to simulate because inputs to only one return are required.

3.5 Auroral Long Path

Scatter functions from auroral paths often show a complex ridge structure indicative of multipath returns from moving ionospheric irregularities. An example of this is in Figure 9a which shows measurements from a 2300-km path between Verona, NY and Frobisher Bay, Canada (Wagner et al., 1989). The measurements were taken near midday in April 1986 under quiet magnetic conditions and substantiates the restless nature of the ionosphere in the auroral zone.

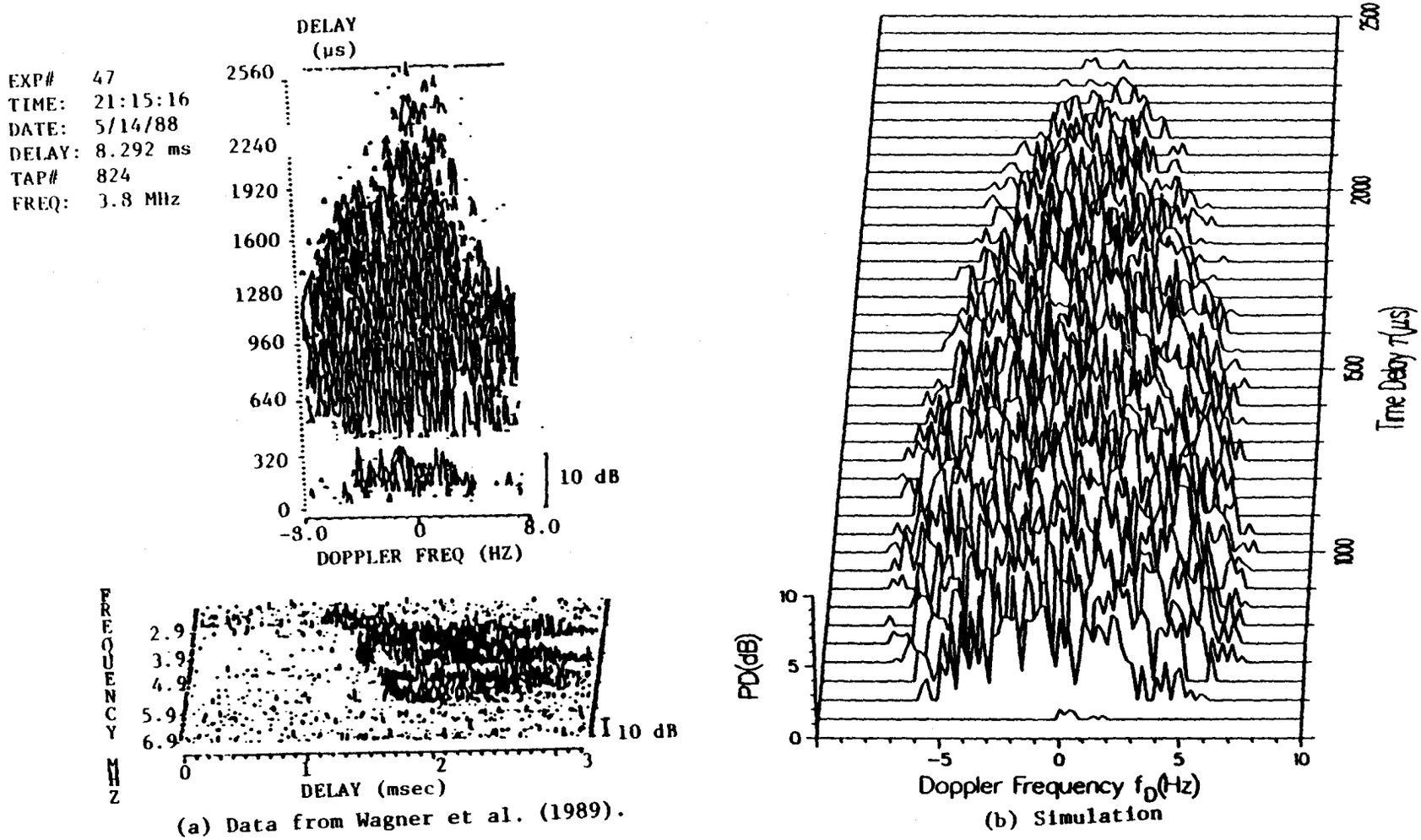

Figure 7. Scatter function from 88-km auroral path during severe spread-F. (a) Lower plot depicts ionogram.

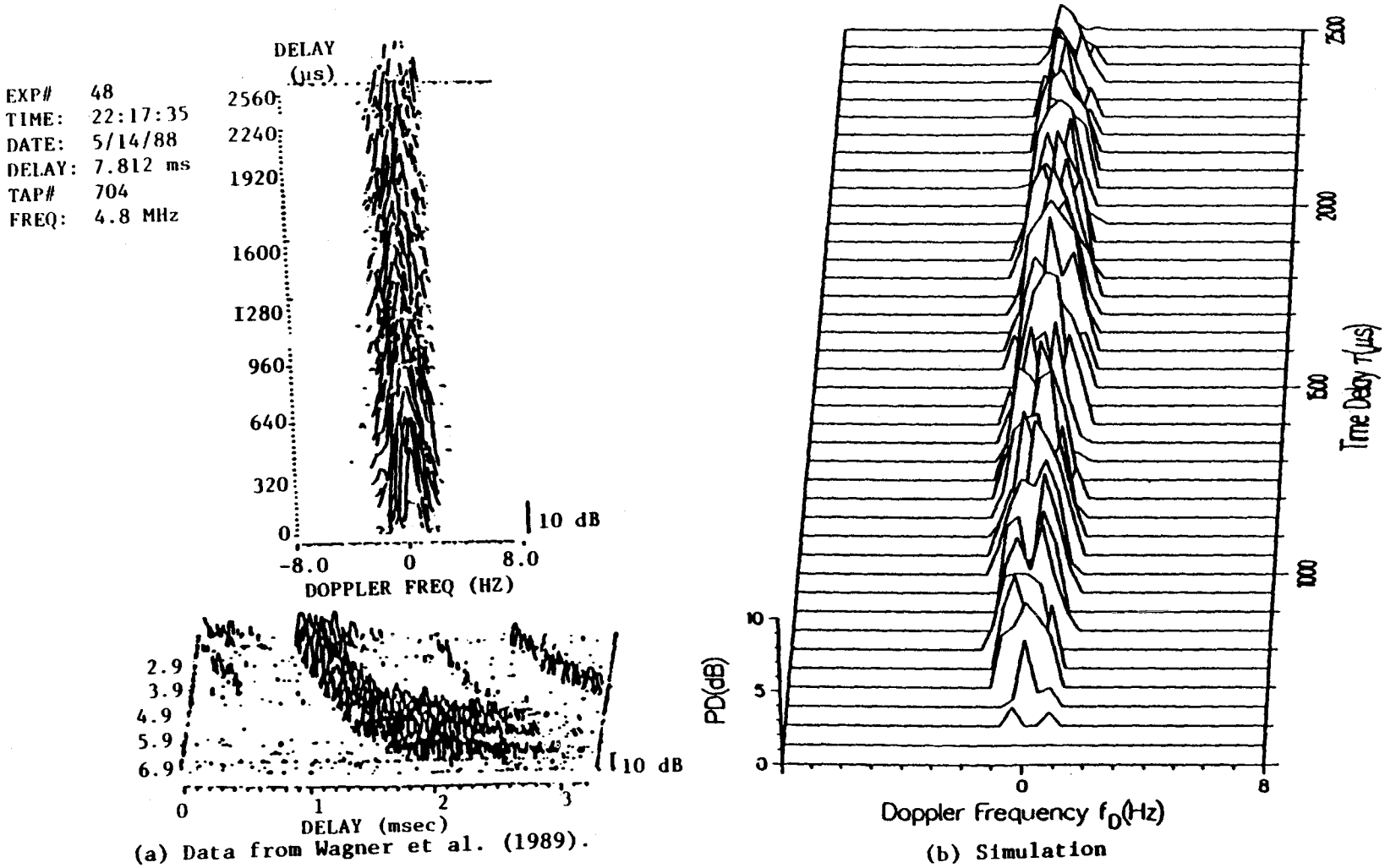

(a) Data from Wagner et al. (1989).

(b) Simulation

Figure 8. Scatter function from same path as Figure 7 during moderate spread-F, 1 hour later. (a) Lower plot depicts ionogram.

Because of the apparent randomness of the motions, it is not possible to duplicate a particular measurement, but Figure 9b shows how the present model can simulate the main features of this type of scatter function. The delay scale in (a) has an arbitrary zero offset. The input parameters (see Table 1 of the Appendix) are chosen more-or-less arbitrarily except for the overall delay and Doppler spreads which are meant to agree with the measured values in Figure 9a. The ridge structure is evident, as it is in the measured plot, but the various pairs of τ, f_D dependencies give an appearance of irregularity.

The difference between using the exponential and the Gaussian correlation factors in simulation is quite noticeable in this example. Figure 9b assumed the exponential factor, whereas the points of Figure 9c were evaluated using the Gaussian shape from (7); all other input was identical in the two cases. From a visual standpoint, the exponential simulation of 9b appears more nearly like the data plot than does 9c. However, a more precise comparison using statistical tests is required for a valid decision, and this matter is reserved for future studies.

3.6 Narrowband Comparison

The limited validity of a narrowband simulation model is graphically illustrated in Figure 10, which compares a scatter function from the present wideband model with an equivalent one that would be obtained from the Watterson narrowband model. The narrowband assumes a bandwidth small enough that dispersion caused by frequency variation is absent and delay spread is negligible; thus, the pulse response has a constant time delay ($\sim$ 8.1 ms in Figure 10b) and no spread.

With a wider bandwidth, dispersion (and scattering) cause the extended delay shown in Figure 10a. In this case values assumed for the stochastic parameters (see Table 1 of the Appendix) were chosen to emphasize the fact that a single profile of the scatter function, such as is obtained by a narrowband model, is insufficient to accurately characterize the response of a wideband system. Therefore, conclusions pertaining to the simulated (narrowband) performance of a modem under these circumstances would be suspect.

4. DISCUSSION AND CONCLUSIONS

The simulation model described in this paper can be structured in either or both of two ways:

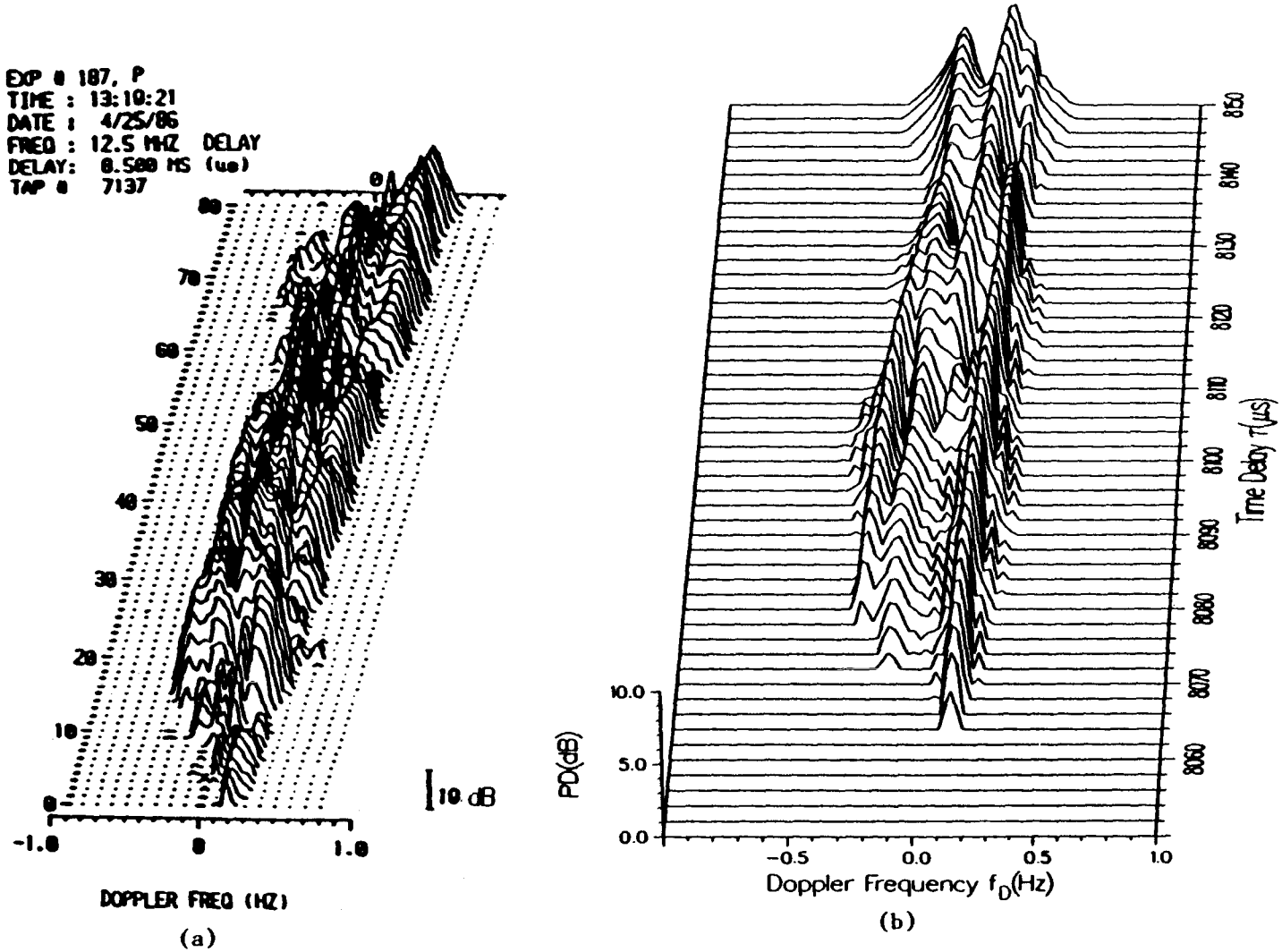

Figure 9. Scatter function from 2300-km auroral path. (a) Data from Wagner et al. (1989). (b) Simulation using exponential correlation factor (eq. (10)).

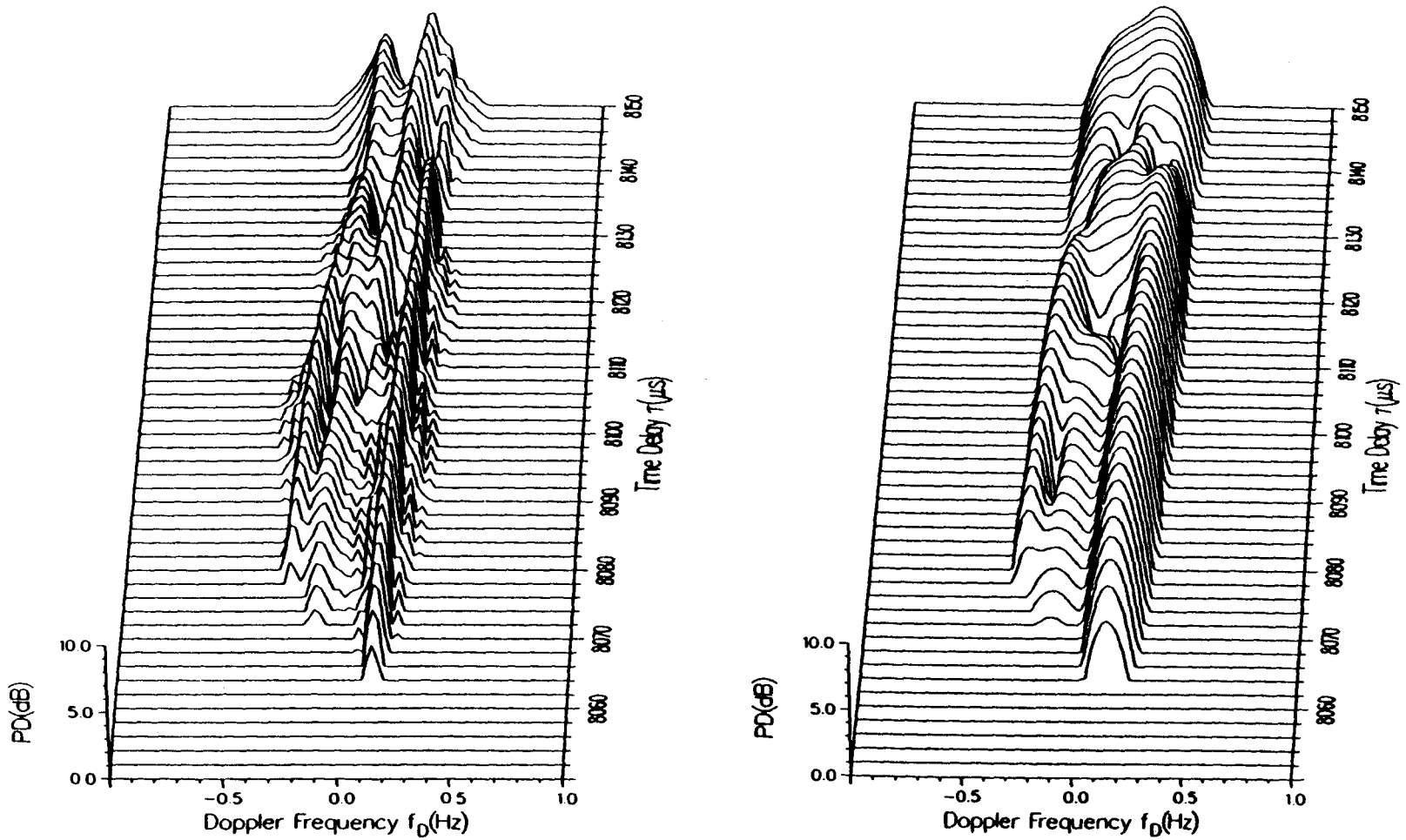

Figure 9c. Scatter functions using the exponential (left) and Gaussian (right) correlation factors. Input parameters are the same as in Figure 9b.

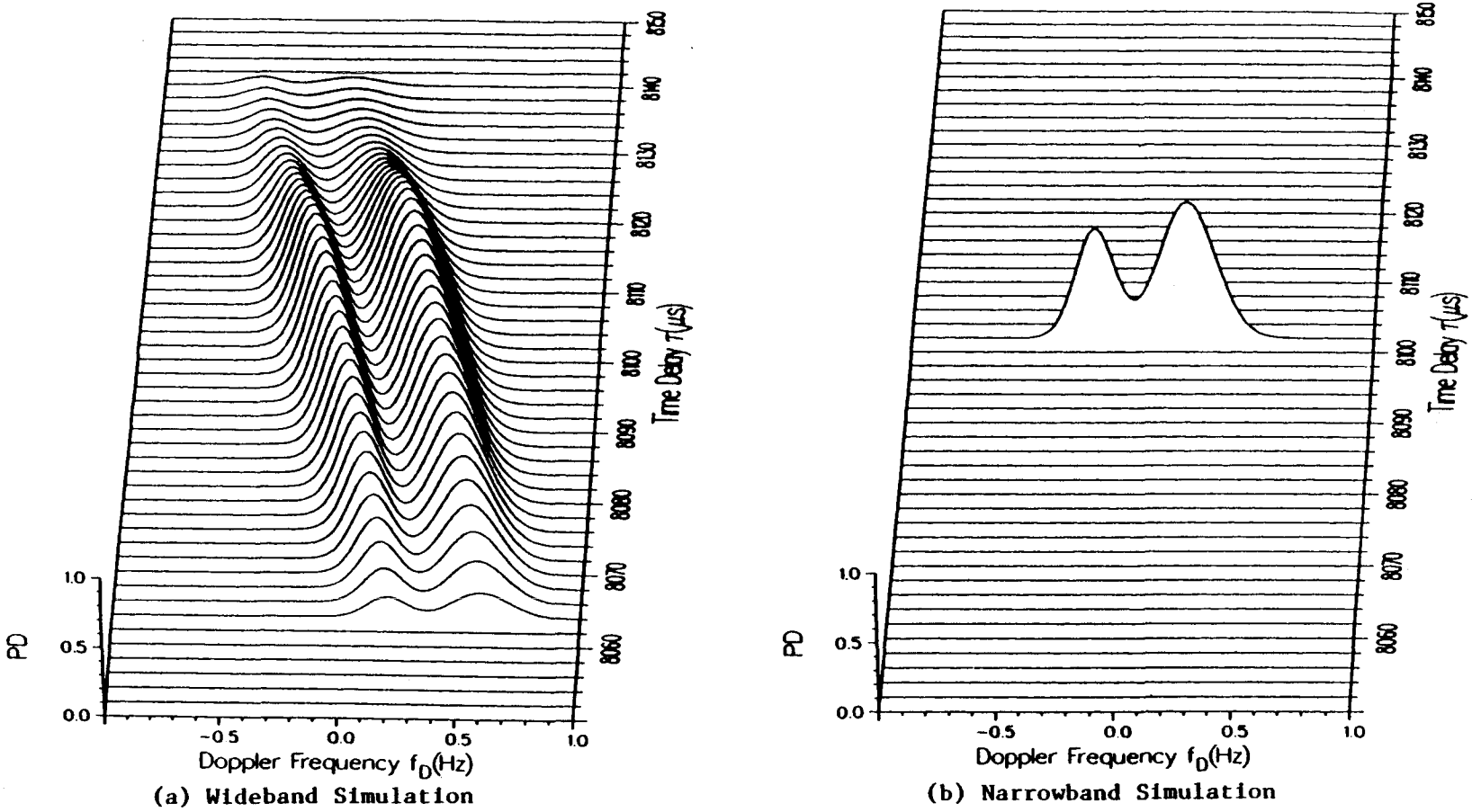

Figure 10. Comparison of scatter functions for a wideband (a) and narrowband (b) simulation model. The bandwidth in (b) is assumed small enough that delay spread is negligible.

A) (Path input). User input consists of path location, seasonal and daily time periods, carrier frequency and bandwidth, and statistical desiderata (e.g., median, 10%, or 90% probability levels). This is used in conjunction with any available HF prediction program to compute values of layer height, thickness, penetration frequency, mode amplitude and extent, and time variability information that is required as parameters for the simulation model (see part B). Note that for a particular layer, the model determines the locations of both the low- and high-rays through (6); i.e., independent input sets of f_p, σ, and h_o are not required for these two rays. In fact it is also possible to account for both ordinary and extraordinary modes from one set of layer values if use is made of the well-known relationship between (geomagnetic) gyro-frequency and ordinary ray penetration frequency [Budden, 1961; p. 208]. Depending on the sophistication of the prediction program, all or only some of the parameters will be calculated and missing values must be entered independently.

B) (Parameter input). User input consists of the parameters listed across the top of Table 1 plus a decision as to the number of modes it is desired to simulate. This manner of entering input can be tedious if more than one mode is desired, however a wide variety of different channel configurations can be investigated this way. Also, of course, the effect of varying just one of the parameters while holding the others constant can be studied.

This report has presented a new ionospheric HF channel model whose output simulates the time-varying properties of the HF sky-wave channel. The mathematical derivation of the model is described and good agreement is found between the model output and empirical data. The channel scattering function is found to be an excellent descriptor of the stochastic time-varying properties of the channel, and therefore is used for the comparisons between the model output and the measured channel propagation data. These comparisons are made for a variety of ionospheric channels including disturbed equatorial and trans-auroral channels - all showing good agreement between the model and the measured data.

The limitations of existing HF channel models are discussed, and it is shown that the new model is valid for much wider bandwidths than existing models. Equally important is the capability of the new model to simulate a wide variety of channels, not just those which may be considered to be stable and stationary. Existing models are able to simulate only stationary channels, and therefore are representative of propagation conditions for only a small portion of the time. Test results obtained from channel simulators based on these restricted channel models must be viewed with some degree of caution. This is true even for tests of narrowband HF communications systems obtained from the use of narrowband HF simulators based on existing HF channel models.

To reach the goal of a general wideband HF channel model capable of simulating all types of propagation channels (not just stationary channels), a more generalized approach to HF channel simulation is required that includes the following:

- simulation of dispersion and scattering from diffuse multipath
- both Gaussian and exponential correlation factors for the tap-gain spectra
- variation of Doppler shift with delay

The stochastic model described in this report, coupled with the deterministic model described in the first report in this series (Vogler and Hoffmeyer, 1988), lays the foundation for a new HF channel simulator which is much more realistic than present channel simulators, even for narrowband applications.

Future work in the development of the new HF channel model and channel simulator based on that model include the following:

- analysis of propagation data tapes to obtain the typical values, ranges, and statistical distributions for the stochastic model parameters described in Section 2
- analysis of propagation data tapes to obtain the assumed shape factors and correlation forms that determine the time delay and Doppler frequency spreads that characterize the channel scattering function
- numerical comparisons of the stochastic model output with measured data
- functional specification of a new wideband channel simulator
- hardware development of a new wideband channel simulator

Data obtained from propagation measurements on a variety of HF sky-wave links will be analyzed to complete the validation of the new model.

In conclusion, it should be noted that the new channel model and the eventual development of a new channel model are not the end objectives of this research program. The end objectives of this program are the testing of new digital HF communications systems that have promising new capabilities for low-probability-of-intercept communications, data throughput, and error performance.

5. ACKNOWLEDGMENTS

The authors wish to thank the Rome Air Development Center for the funding support for this project and Mr. J. McEvoy of RADC for suggestions he has made during the course of this research project. We also thank Mr. D. Bodson and G. Rekstad of the National Communications System for their support of this project. Finally, we thank Dr. L. Wagner of the Naval Research Laboratory and Mr. R. Basler for permission to use selected plots of measured propagation data for comparison with plots from the model described in this report.

6. REFERENCES

Barratt, J.J., and T.L. Walton (1987), A real-time wideband propagation simulator for the high frequency band, Ionospheric Effects Symp., Naval Research Laboratory, Washington, DC, pp. 9 - 20.

Basler, R.P., P.B. Bentley, G.H. Price, R.T. Tsunoda, and T.L. Wong (1987a), Ionospheric distortion of HF signals, Tech. Report DNA-TR-87-246, SRI Project 8675, SRI International, Menlo Park, CA 94025.

Basler, R.P., G.H. Price, R.T. Tsunoda, and T.L. Wong (1987b), HF channel probe, Ionospheric Effects Symp., Naval Research Laboratory, Washington, DC, pp. 1-8.

Basler, R.P., G.H. Price, R.T. Tsunoda, and T.L. Wong (1988), Ionospheric distortion of HF signals, Radio Science 23, No. 4, pp. 569-579.

Belknap, D.J., R. D. Haggarty, and B. D. Perry (1968), Adaptive signal processing for ionospheric distortion correction, Mitre Tech. Rpt. 746, Mitre Corp. Bedford, MA, August.

Bello, P. and F. Fishman (1989), Evaluation of wideband HF signal detection techniques by partially processed noise measurements, Military Commun. Conf., Boston, Paper No. 35.5.

Budden, K.G., (1961), Radio Waves in the Ionosphere, (Cambridge University Press, New York, NY).

Campbell, G.A., and R.M. Foster (1948), Fourier Interals for Practical Applications, (D. Van Nostrand, Princeton, NJ).

CCIR (1974), HF ionospheric channel simulators, XIIIth Plenary Assembly, ITU, Geneva, Switzerland, Vol. III, Report 549, pp. 66-72.

CCIR (1986), HF ionospheric channel simulators, XVth Plenary Assembly, ITU, Dubrovnik, Vol. III, Report 549-2, pp. 59-67.

Dixon, R.C. (1984), Spread Spectrum Systems, (John Wiley and Sons, New York, NY).

Ehrman, L., L.B. Bates, J.F. Eschle, and J.M. Kates (1982), Real-time software simulation of the HF radio channel, IEEE Trans. Commun., COM-30, No. 8, pp.1809-1817, Aug.

Girault, R., J. Thibault, and B. Durand (1988), Software ionospheric channel simulator, IEE Fourth Intl. Conf. on HF Radio Systems and Techniques, London UK, IEE Pub. 284, pp. 321-325.

Hoffmeyer, J.A., and M. Nesenbergs (1987), Wideband HF modeling and simulation, NTIA Report 87-221, Jul., NTIS* Order No. PB 88-116116/AS).

Lemmon, J.J. (1989), Wideband HF noise and interference modeling, IEEE 1989 Military Commun. Conf., Boston, October, Paper No. 48.4.

LeRoux, Y.M., G. Savidan, G. DuChaffaut, P. Gourvez, and J.P. Jolivet (1987), A combined evaluation and simulation system of the HF channel, IEE Fifth Intl. Conf. on Ant. and Prop., York, UK, IEE Pub. 274, pp. 171-175.

McRae, D.D., and F.A. Perkins (1988), Digital HF modem performance measurements using HF link simulators, IEE Fourth Intl. Conf. on HF Radio Systems and Techniques, London, UK, IEE Pub. 284, pp. 314-317.

Mihram, G.A. (1972), Simulation: Statistical Foundations and Methodology, (Academic Press, New York, NY).

Milsom, J.D., and T. Slator (1982), Consideration of factors influencing the use of spread spectrum on HF sky-wave paths, Second Conf. on HF Commun. Systems and Techniques, London, IEE Publication No. 206, pp. 71-74.

Mooney, O.J. (1985), Implementation of an HF ionospheric channel simulator using a digital signal processor, IEE Third Intl. Conf. on HF Commun. Systems and Techniques, London, UK, pp. 27-31.

Naylor, T.H., J.L. Balintfy, D.S. Burdick, and K. Chu (1966), Computer Simulation Techniques, (John Wiley & Sons, New York, NY)

Perry, B. D. (1983), A new wideband HF technique for MHz-bandwidth spreadspectrum radio communications," IEEE Commun. Mag., 21, No. 6., Sept., pp 28-36

---

* National Technical Information Service, 5285 Port Royal Rd., Springfield, VA 22161

Perry, B.D., E.A. Palo, R.D. Haggarty, and E.L. Key (1987), Trade-off considerations in the use of wideband HF communications, IEEE Intl. Conf. Commun., Seattle, WA, Paper No. 26.2.

Proakis, J.G. (1983), Digital Communications, (McGraw - Hill, New York, NY).

Salous, S., and E.D. Shearman (1986), Wideband measurements of coherence over an HF skywave link and implication for spread-spectrum communication, Radio Sci. 21, No. 3, pp. 463-472, May-Jun.

Serrat-Fernandez, J., J.A. Delgado-Penin, E. Munday, and P.G. Farrell (1985), Measurement and verification of an HF channel model, IEE Third Intl. Conf. on HF Commun. Systems and Techniques, London, UK, IEE Pub. 245, pp. 52-56.

Skaug, R. (1982), An experiment with spread spectrum modulation on an HF channel, IEE Second Conf. on HF Commun. Systems and Techniques, London, UK, IEE Pub. 206, pp. 76-80.

Skaug, R. (1984), Experiment with spread spectrum modulation on an HF channel, IEE Proc. 131, Part F, No. 1, Feb., pp. 87-91.

Vogler, L.E., and J.A. Hoffmeyer (1988), A new approach to HF channel modeling and simulation, Part 1: Deterministic model, NTIA Report 88-240, Dec., (NTIS Order No. PB89-203962/AS).

Wagner, L.S. (1987), Characteristics of mid-latitude sporadic E observed with a wideband HF channel probe, Radio Sci.22, No. 5, pp. 728-744, Sept.-Oct.

Wagner, L.S., and J.A. Goldstein (1985), High-resolution probing of the HF ionospheric skywave channel: F_2 layer results, Radio Sci. 20, No. 3, pp. 287-302, May-Jun.

Wagner, L.S., J.A. Goldstein, and E.A. Chapman (1983), Wideband HF channel prober: system description, Tech. Report, Naval Research Laboratory, Washington, DC, Mar.

Wagner, L.S., J.A. Goldstein, and W.D. Meyers (1987a), Wideband probing of the trans-auroral HF channel, IEEE 1987 Military Commun. Conf., Washington, DC, Paper No. 43.2.

Wagner, L.S., J.A. Goldstein, and W.D. Meyers (1987b), Wideband probing of the trans-auroral HF channel: solar minimum, Ionospheric Effects Symp., Naval Research Laboratory, Washington, DC, pp. 31-43.

Wagner, L.S., J.A. Goldstein, and W.D. Myers (1988), Wideband probing of the transauroral HF channel: solar minimum, Radio Science 23, No. 4, pp. 555-568.

Wagner, L.S., J.A. Goldstein, W.D. Meyers, and P.A. Bello (1989), The HF skywave channel: measured scattering functions for midlatitude and auroral channels and estimates for short-term wideband HF rake modem performance, MILCOM '89 Conf. Record, Vol. 3, pp. 482.1 - 48.2.10, 1989 IEEE Military Commun. Conf., Boston, Mass.

Watterson, C.C. (1981), HF channel-simulator measurements on the KY-870/P FSK burst-communication modem-set 1, NTIA Report CR-81-13, (NTIS* Order No. PB 82-118944).

Watterson, C.C. (1982), HF channel-simulator measurements on the KY-879/P FSK burst-communication modem-set 2, NTIA Contractor Report CR-82-20, Dec., (NTIS* Order No. PB 83-194738).

Watterson, C.C. and R.M. Coon (1969), Recommended specifications for ionospheric noise simulators, ESSA Tech. Report ERL-127-ITS-89.

Watterson, C.C., J.R. Juroshek, and W.D. Bensema (1969), Experimental verification of an ionospheric channel model, ESSA Tech. Report ERL 112-ITS 80.

Watterson, C.C., J.R. Juroshek, and W.D. Bensema (1970), Experimental confirmation of an HF channel model, IEEE Trans. Commun. Technol. COM-18, pp. 792-803.

Wright, J.W. and R.W. Knecht (1957), The IGY 1957-1958 atlas of ionograms, Special CRPL Publication, National Bureau of Standards (Boulder, CO).

---

* National Technical Information Service, 5285 Port Royal Rd., Springfield, VA 22161

Appendix

Table 1 displays input values that were used to generate the simulated scatter functions of Figures 4-10. The path distance D and carrier frequency f_c are given in the first two columns after the figure numbers. The number of modes simulated in any particular figure can be determined from the number of entries of the layer parameters f_p, σ, and h_o; e.g., there is one mode in Figure 4 and three modes in Figure 6. Each mode has both low- and high-ray input values for the delay and Doppler spread parameters in the last six columns. If the high-ray is not present in the simulation, this is indicated by a row of zeroes. The amplitude A is a dimensionless factor that can range from zero to unity.

Table 1. Parameters used in the simulation model for Figures 4 - 10.

	D (km)	f_c (MHz)	f_p (MHz)	σ (km)	h_o (km)	A	σ_τ (μs)	σ_c (μs)	σ_D (Hz)	fs (Hz)	fsL (Hz)
Fig. 4	2158	11	7.2	56.7	472	1	880	220	2	0	0
						0	0	0	0	0	0
Fig. 5	1913	12.5	5.72	19.22	306.8	0.34	250	135	7	0	0
						0	0	0	0	0	0
			5.72	19.22	364.5	0.84	400	100	16	0	0
						0.44	945	135	22	0	0
Fig. 6	126	5.5	13	30	265	1	70	35	0.05	0.2	0.1
						0	0	0	0	0	0
			13	28	271.5	1	30	15	0.1	0.05	-0.05
						0	0	0	0	0	0
			13	28	270	1	20	10	0.05	-0.1	0
						0	0	0	0	0	0
Fig. 7	88	3.8	7	30	235	1	1900	400	8	0	0
						0	0	0	0	0	0
Fig. 8	88	4.8	7	30	235	1	2200	1000	1.5	0	0
						0	0	0	0	0	0
Fig. 9	2300	12.5	4.25	8.43	374	1	100	40	0.15	0.2	0.1
						0.5	100	50	0.2	0.2	0
			4.25	8.43	374	0.5	60	25	0.1	-0.2	-0.3
						0.3	100	80	0.2	0	-0.1
Fig. 10	2300	12.5	4.25	8.43	374	1	80	40	0.3	0.2	0.6
						0	0	0	0	0	0
			4.25	8.43	374	0.8	80	40	0.2	-0.2	0.2
						0	0	0	0	0	0

FORM **NTIA-29**
(4-80)

U.S. DEPARTMENT OF COMMERCE
NAT'L. TELECOMMUNICATIONS AND INFORMATION ADMINISTRATION

BIBLIOGRAPHIC DATA SHEET

	1. PUBLICATION NO.	2. Gov't Accession No.	3. Recipient's Accession No.

4. TITLE AND SUBTITLE

A New Approach to HF Channel Modeling and Simulation
Part II: Stochastic Model

5. Publication Date
February 1990

6. Performing Organization Code
NTIA/ITS

7. AUTHOR(S)
L.E. Vogler and J.A. Hoffmeyer

9. Project/Task/Work Unit No.

8. PERFORMING ORGANIZATION NAME AND ADDRESS
National Telecommunications & Information Administration
Institute for Telecommunication Sciences
325 Broadway
Boulder, CO 80303

10. Contract/Grant No.

11. Sponsoring Organization Name and Address
Dept. of the Air Force, Rome Air Development Center
Griffiss AFB, NY 13441-5700

12. Type of Report and Period Covered

13.

14. SUPPLEMENTARY NOTES

15. ABSTRACT *(A 200-word or less factual summary of most significant information. If document includes a significant bibliography or literature survey, mention it here.)*

This report is the second report in a series of reports which describe a new and unique approach for modeling either narrowband or wideband high frequency (HF) channels. Although narrowband models of the HF channel have existed for many years, they are applicable to only a limited set of actual narrowband propagation conditions. The need for an HF channel model that is valid for both narrow and wide bandwidths over a more extensive range of propagation conditions motivated the research documented in this series of reports.

Continued on reverse

16. Key Words *(Alphabetical order, separated by semicolons)*

channel transfer function, HF channel models; HF propagation; scattering functions; spread spectrum communications; wideband HF

17. AVAILABILITY STATEMENT

☒ UNLIMITED.

☐ FOR OFFICIAL DISTRIBUTION.

18. Security Class. *(This report)*
unclassified

20. Number of pages
37

19. Security Class. *(This page)*
unclassified

21. Price:

☆ U.S. Government Printing Office: 1980—678-495/529

15. ABSTRACT (continued)

The reports in this series describe the development of a channel transfer function for the HF channel that accurately models a wide variety of propagation conditions and can be used for the evaluation of either narrowband or wideband HF systems. Part I of this series of reports described the development of a model that represents the median channel conditions. The present report, Part II of the series, describes the stochastic portion of the model which simulates the time-varying distortion of a transmitted signal due to dispersion, scattering due to irregularities in the ionosphere, Doppler spread and Doppler shift. The development of the stochastic model is described. The model output is compared with measured propagation data obtained on a variety of HF links. The mechanism for this comparison is the channel scattering function which has been found to be an excellent descriptor of the time-varying dispersive HF channel.

☆ U.S. GOVERNMENT PRINTING OFFICE: 1990—773-002/11,030 REGION NO. 8